Available online at www.sciencedirect.com
SCIENCE DIRECT®
ELSEVIER
International Journal of Solids and Structures 42 (2005) 4641–4662
INTERNATIONAL JOURNAL OF SOLIDS and STRUCTURES
www.elsevier.com/locate/ijsolstr

Postbuckling of FGM cylindrical shells under combined axial and radial mechanical loads in thermal environments

Hui-Shen Shen [a,*], N. Noda [b]

[a] School of Ocean and Civil Engineering, Shanghai Jiao Tong University, Shanghai 200030, People's Republic of China
[b] Department of Mechanical Engineering, Shizuoka University, Johoku 3-5-1, Hamamatsu 432-8561, Japan

Received 13 August 2004; received in revised form 8 February 2005
Available online 17 March 2005

Abstract

A postbuckling analysis is presented for a shear deformable functionally graded cylindrical shell of finite length subjected to combined axial and radial loads in thermal environments. Heat conduction and temperature-dependent material properties are both taken into account. The temperature field considered is assumed to be a uniform distribution over the shell surface and varied in the thickness direction only. Material properties are assumed to be temperature-dependent, and graded in the thickness direction according to a simple power law distribution in terms of the volume fractions of the constituents. The formulations are based on a higher order shear deformation shell theory with von Kármán–Donnell-type of kinematic nonlinearity. A boundary layer theory of shell buckling, which includes the effects of nonlinear prebuckling deformations, large deflections in the postbuckling range, and initial geometric imperfections of the shell, is extended to the case of functionally graded cylindrical shells. A singular perturbation technique is employed to determine the interactive buckling loads and postbuckling equilibrium paths. The numerical illustrations concern the postbuckling response of perfect and imperfect cylindrical shells with two constituent materials subjected to combined axial and radial mechanical loads and under different sets of thermal environments. The results reveal that the temperature field and volume fraction distribution have a significant effect on the postbuckling behavior, but they have a small effect on the imperfection sensitivity of the functionally graded shell.

Keywords: Functionally graded material; Heat conduction; Temperature-dependent properties; Cylindrical shell; Postbuckling; Combined loading

* Corresponding author.
E-mail address: hsshen@mail.sjtu.edu.cn (H.-S. Shen).

0020-7683/$ - see front matter © 2005 Elsevier Ltd. All rights reserved.
doi:10.1016/j.ijsolstr.2005.02.005

1. Introduction

Recently, a new class of composite materials known as functionally graded materials (FGMs) has drawn considerable attention. Typically, FGMs are made from a mixture of metals and ceramics and are further characterized by a smooth and continuous change of the mechanical properties from one surface to another. It has been reported that the weakness of the fiber reinforced laminated composite materials, such as debonding, huge residual stress, locally largely plastic deformations, etc., can be avoided or reduced in FGMs (Noda, 1991; Tanigawa, 1995). Hence, FGMs are possessed of an enormous application potential, especially for working in the high temperature environments. With the increased usage of these materials, it is important to understand the buckling and postbuckling behaviors of FGM cylindrical shells subjected to mechanical loads in thermal environments.

Many initial postbuckling or fully nonlinear postbuckling studies of isotropic and composite laminated cylindrical shells have been performed by the classical and/or shear deformation shell theory. However, investigations on the buckling and postbuckling analysis of FGM cylindrical shells under thermal or mechanical loading are limited in number. Shahsiah and Eslami (2003a,b) presented the buckling temperature of simply supported FGM cylindrical shells under two cases of thermal loading, i.e. uniform temperature rise, linear and nonlinear gradient through the thickness, based on the first order shear deformation shell theory. In their analysis the material properties were considered to be independent of temperature. Shen (2002, 2003) studied the buckling and postbuckling of FGM cylindrical thin shells subjected to axial compression or lateral pressure in thermal environments. In the above studies, the material properties were considered to be temperature-dependent and the effect of temperature rise on the postbuckling behavior was reported. Recently, Shen (2004) gave a thermal postbuckling analysis of FGM cylindrical thin shells subjected to a uniform temperature rise. It should be noted that in the above studies the shells are considered as being relatively thin and therefore the transverse shear deformation is usually not accounted for. On the other hand, ceramics and the metals used in FGM do store different amounts of heat. This leads to a non-uniform distribution of temperature through the plate thickness, especially when the plate is thick. Hence the heat conduction usually occurs (Tanigawa et al., 1996; Kim and Noda, 2002), but it is not accounted for in the above studies. This is because when the material properties are assumed to be functions of temperature and position, and the temperature is also assumed to be a function of position, the problem becomes very difficult.

The present work attempts to solve this problem, that is, to provide analytical solution for the postbuckling of FGM cylindrical shell of finite length subjected to combined axial and radial loads in thermal environments. Heat conduction and temperature-dependent material properties are both taken into account. The temperature field considered is assumed to be a uniform distribution over the shell surface and varied in the thickness direction only. Material properties are assumed to be temperature-dependent, and graded in the thickness direction according to a simple power law distribution in terms of the volume fractions of the constituents. The formulations are based on Reddy's higher order shear deformation shell theory with von Kármán–Donnell-type of kinematic nonlinearity and including thermal effects. The boundary layer theory suggested by Shen and Chen (1988, 1990) is extended to the case of FGM cylindrical shells of finite length. A singular perturbation technique is employed to determine the interactive buckling loads and postbuckling equilibrium paths. The nonlinear prebuckling deformations and initial geometric imperfections of the shell are both taken into account but, for simplicity, the form of initial geometric imperfection is assumed to be the same as the initial buckling mode of the shell. The numerical illustrations show the full nonlinear postbuckling response of FGM cylindrical shells subjected to combined axial and radial mechanical loads and under different sets of environmental conditions.

2. Theoretical development

Consider an FGM circular cylindrical shell with mean radius R, length L and thickness t, which is made from a mixture of ceramics and metals. The shell is referred to a coordinate system (X, Y, Z) in which X and Y are in the axial and circumferential directions of the shell and Z is in the direction of the inward normal to the middle surface. The corresponding displacement are designated by $\overline{U}$, $\overline{V}$ and $\overline{W}$. $\overline{\Psi}_x$ and $\overline{\Psi}_y$ are the rotations of the normals to the middle surface with respect to the Y- and X-axes, respectively. The origin of the coordinate system is located at the end of the shell on the middle plane. The shell is assumed to be geometrically imperfect, exposed to elevated temperature, and subjected to two loads combined out of a uniform external pressure q and axial load P. Denoting the initial geometric imperfection by $\overline{W}^*(X, Y)$, let $\overline{W}$ (X, Y) be the additional deflection and $\overline{F}(X, Y)$ be the stress function for the stress resultants defined by $\overline{N}_x = \overline{F}_{,yy}$, $\overline{N}_y = \overline{F}_{,xx}$ and $\overline{N}_{xy} = -\overline{F}_{,xy}$, where a comma denotes partial differentiation with respect to the corresponding coordinates.

We assume that the composition is varied from the outer to the inner surface, i.e. the outer surface $(Z = -t/2)$ of the shell is ceramic-rich whereas the inner surface $(Z = t/2)$ is metal-rich. In such a way, the effective material properties P, like Young's modulus E or thermal expansion coefficient α, can be expressed as

$$P = P_c V_c + P_m V_m \tag{1}$$

in which P_c and P_m denote the temperature-dependent properties of the ceramic and metal, respectively, and may be expressed as a function of temperature (Touloukian, 1967)

$$P = P_0(P_{-1}T^{-1} + 1 + P_1 T + P_2 T^2 + P_3 T^3) \tag{2}$$

in which $T = T_0 + \Delta T$ and $T_0 = 300$ K (room temperature), P_0, P_{-1}, P_1, P_2 and P_3 are the coefficients of temperature T (K) and are unique to the constituent materials.

V_c and V_m are the ceramic and metal volume fractions and are related by

$$V_c + V_m = 1 \tag{3}$$

and we assume the volume fraction V_m follows a simple power law as

$$V_m = \left(\frac{2Z + t}{2t}\right)^N \tag{4}$$

where the volume fraction index N dictates the material variation profile through the shell panel thickness and may be varied to obtain the optimum distribution of component materials.

It is assumed that the effective Young's modulus E and thermal expansion coefficient α are temperature-dependent, whereas the thermal conductivity κ is independent to the temperature. Poisson's ratio ν depends weakly on temperature change and is assumed to be a constant. From Eqs. (1)–(4), one has

$$E(Z, T) = [E_c(T) - E_m(T)]\left(\frac{2Z + t}{2t}\right)^N + E_m(T) \tag{5a}$$

$$\alpha(Z, T) = [\alpha_c(T) - \alpha_m(T)]\left(\frac{2Z + t}{2t}\right)^N + \alpha_m(T) \tag{5b}$$

$$\kappa(Z) = (\kappa_c - \kappa_m)\left(\frac{2Z + t}{2t}\right)^N + \kappa_m \tag{5c}$$

We assume that the temperature variation occurs in the thickness direction only and one dimensional temperature field is assumed to be constant in the XY plane of the shell. In such a case, the temperature distribution along the thickness can be obtained by solving a steady-state heat transfer equation

$$-\frac{\mathrm{d}}{\mathrm{d}Z}\left[\kappa(Z)\frac{\mathrm{d}T}{\mathrm{d}Z}\right]=0 \tag{6}$$

This equation is solved by imposing boundary condition of $T=T_{\mathrm{U}}$ at $Z=-t/2$ and $T=T_{\mathrm{L}}$ at $Z=t/2$. The solution of this equation, by means of polynomial series, is

$$T(Z)=T_{\mathrm{U}}+(T_{\mathrm{L}}-T_{\mathrm{U}})\eta(Z) \tag{7}$$

and

$$\eta(Z)=\frac{1}{C}\left[\left(\frac{2Z+t}{2t}\right)-\frac{\kappa_{\mathrm{mc}}}{(N+1)\kappa_{\mathrm{c}}}\left(\frac{2Z+t}{2t}\right)^{N+1}+\frac{\kappa_{\mathrm{mc}}^2}{(2N+1)\kappa_{\mathrm{c}}^2}\left(\frac{2Z+t}{2t}\right)^{2N+1}-\frac{\kappa_{\mathrm{mc}}^3}{(3N+1)\kappa_{\mathrm{c}}^3}\left(\frac{2Z+t}{2t}\right)^{3N+1}+\frac{\kappa_{\mathrm{mc}}^4}{(4N+1)\kappa_{\mathrm{c}}^4}\left(\frac{2Z+t}{2t}\right)^{4N+1}-\frac{\kappa_{\mathrm{mc}}^5}{(5N+1)\kappa_{\mathrm{c}}^5}\left(\frac{2Z+t}{2t}\right)^{5N+1}\right] \tag{8a}$$

$$C=1-\frac{\kappa_{\mathrm{mc}}}{(N+1)\kappa_{\mathrm{c}}}+\frac{\kappa_{\mathrm{mc}}^2}{(2N+1)\kappa_{\mathrm{c}}^2}-\frac{\kappa_{\mathrm{mc}}^3}{(3N+1)\kappa_{\mathrm{c}}^3}+\frac{\kappa_{\mathrm{mc}}^4}{(4N+1)\kappa_{\mathrm{c}}^4}-\frac{\kappa_{\mathrm{mc}}^5}{(5N+1)\kappa_{\mathrm{c}}^5} \tag{8b}$$

where $\kappa_{\mathrm{mc}}=\kappa_{\mathrm{m}}-\kappa_{\mathrm{c}}$. In particular, for an isotropic material, Eq. (7) may then be expressed as

$$T(Z)=\frac{T_{\mathrm{U}}+T_{\mathrm{L}}}{2}+\frac{T_{\mathrm{L}}-T_{\mathrm{U}}}{t}Z \tag{9}$$

From Eqs. (5a), (5b) and (7), it can be seen that now E_{c}, E_{m}, α_{c} and α_{m} are all functions of temperature and position.

Reddy and Liu (1985) developed a simple higher order shear deformation shell theory, in which the transverse shear strains are assumed to be parabolically distributed across the shell thickness and which contains the same number of dependent unknowns as in the first order shear deformation theory. Based on Reddy's higher order shear deformation theory with a von Kármán–Donnell-type of kinematic nonlinearity and including thermal effects, the governing differential equations for an FGM cylindrical shell can be derived in terms of a stress function $\overline{F}$, two rotations $\overline{\Psi}_x$ and $\overline{\Psi}_y$, and a transverse displacement $\overline{W}$, along with the initial geometric imperfection $\overline{W}^*$. They are

$$\widetilde{L}_{11}(\overline{W})-\widetilde{L}_{12}(\overline{\Psi}_x)-\widetilde{L}_{13}(\overline{\Psi}_y)+\widetilde{L}_{14}(\overline{F})-\widetilde{L}_{15}(\overline{N}^{\mathrm{T}})-\widetilde{L}_{16}(\overline{M}^{\mathrm{T}})-\frac{1}{R}\overline{F}_{,xx}=\widetilde{L}(\overline{W}+\overline{W}^*,\overline{F}) \tag{10}$$

$$\widetilde{L}_{21}(\overline{F})+\widetilde{L}_{22}(\overline{\Psi}_x)+\widetilde{L}_{23}(\overline{\Psi}_y)-\widetilde{L}_{24}(\overline{W})-\widetilde{L}_{25}(\overline{N}^{\mathrm{T}})+\frac{1}{R}\overline{W}_{,xx}=-\frac{1}{2}\widetilde{L}(\overline{W}+2\overline{W}^*,\overline{W}) \tag{11}$$

$$\widetilde{L}_{31}(\overline{W})+\widetilde{L}_{32}(\overline{\Psi}_x)-\widetilde{L}_{33}(\overline{\Psi}_y)+\widetilde{L}_{34}(\overline{F})-\widetilde{L}_{35}(\overline{N}^{\mathrm{T}})-\widetilde{L}_{36}(\overline{S}^{\mathrm{T}})=0 \tag{12}$$

$$\widetilde{L}_{41}(\overline{W})-\widetilde{L}_{42}(\overline{\Psi}_x)+\widetilde{L}_{43}(\overline{\Psi}_y)+\widetilde{L}_{44}(\overline{F})-\widetilde{L}_{45}(\overline{N}^{\mathrm{T}})-\widetilde{L}_{46}(\overline{S}^{\mathrm{T}})=0 \tag{13}$$

where all the linear operators $\widetilde{L}_{ij}(\ )$ and the nonlinear operator $\widetilde{L}(\ )$ are defined as in Shen and Li (2002).

The forces $\overline{N}^{\mathrm{T}}$, moments $\overline{M}^{\mathrm{T}}$ and higher-order moments $\overline{P}^{\mathrm{T}}$ caused by elevated temperature are defined by

$$\begin{bmatrix} \overline{N}_x^{\mathrm{T}} & \overline{M}_x^{\mathrm{T}} & \overline{P}_x^{\mathrm{T}} \\ \overline{N}_y^{\mathrm{T}} & \overline{M}_y^{\mathrm{T}} & \overline{P}_y^{\mathrm{T}} \\ \overline{N}_{xy}^{\mathrm{T}} & \overline{M}_{xy}^{\mathrm{T}} & \overline{P}_{xy}^{\mathrm{T}} \end{bmatrix} = \int_{-t/2}^{t/2} \begin{bmatrix} A_x \\ A_y \\ A_{xy} \end{bmatrix} (1, Z, Z^3)\Delta T(Z)\,\mathrm{d}Z \tag{14a}$$

$$\begin{bmatrix} \overline{S}_x^{\mathrm{T}} \\ \overline{S}_y^{\mathrm{T}} \\ \overline{S}_{xy}^{\mathrm{T}} \end{bmatrix} = \begin{bmatrix} \overline{M}_x^{\mathrm{T}} \\ \overline{M}_y^{\mathrm{T}} \\ \overline{M}_{xy}^{\mathrm{T}} \end{bmatrix} - \frac{4}{3t^2} \begin{bmatrix} \overline{P}_x^{\mathrm{T}} \\ \overline{P}_y^{\mathrm{T}} \\ \overline{P}_{xy}^{\mathrm{T}} \end{bmatrix} \tag{14b}$$

where $\Delta T = T(Z) - T_0$ is temperature rise from some reference temperature T_0 at which there are no thermal strains, and

$$\begin{bmatrix} A_x \\ A_y \\ A_{xy} \end{bmatrix} = -\begin{bmatrix} Q_{11} & Q_{12} & Q_{16} \\ Q_{12} & Q_{22} & Q_{26} \\ Q_{16} & Q_{26} & Q_{66} \end{bmatrix} \begin{bmatrix} 1 & 0 \\ 0 & 1 \\ 0 & 0 \end{bmatrix} \begin{bmatrix} \alpha(Z,T) \\ \alpha(Z,T) \end{bmatrix} \tag{15}$$

where the thermal expansion coefficient α is given in detail in Eq. (5b), and

$$Q_{11} = Q_{22} = \frac{E(Z,T)}{1-\nu^2}, \quad Q_{12} = \frac{\nu E(Z,T)}{1-\nu^2}, \quad Q_{16} = Q_{26} = 0, \quad Q_{66} = \frac{E(Z,T)}{2(1+\nu)} \tag{16}$$

in which E is also given in detail in Eq. (5a).

The two end edges of the shell are assumed to be simply supported or clamped, so that the boundary conditions are$X = 0$, L:

$$\overline{W} = \overline{\Psi}_y = 0, \overline{M}_x = \overline{P}_x = 0 \quad \text{(simply supported)} \tag{17a}$$

$$\overline{W} = \overline{\Psi}_x = \overline{\Psi}_y = 0 \quad \text{(clamped)} \tag{17b}$$

$$\int_0^{2\pi R} \overline{N}_x\,\mathrm{d}Y + 2\pi R t\sigma_x + \pi R^2 q a = 0 \tag{17c}$$

where $a = 0$ and $a = 1$ for lateral and hydrostatic pressure loading case, respectively, and σ_x is the average axial compressive stress, and $\overline{M}_x$ is the bending moment, $\overline{P}_x$ is the higher-order moment as defined in Reddy and Liu (1985). Also, we have the closed (or periodicity) condition

$$\int_0^{2\pi R} \frac{\partial \overline{V}}{\partial Y}\,\mathrm{d}Y = 0 \tag{18a}$$

or

$$\int_0^{2\pi R} \left[\left(A_{22}^* \frac{\partial^2 \overline{F}}{\partial X^2} + A_{12}^* \frac{\partial^2 \overline{F}}{\partial Y^2} \right) + \left(B_{21}^* - \frac{4}{3t^2} E_{21}^* \right) \frac{\partial \overline{\Psi}_x}{\partial X} + \left(B_{22}^* - \frac{4}{3t^2} E_{22}^* \right) \frac{\partial \overline{\Psi}_y}{\partial Y} - \frac{4}{3t^2} \left(E_{21}^* \frac{\partial^2 \overline{W}}{\partial X^2} + E_{22}^* \frac{\partial^2 \overline{W}}{\partial Y^2} \right) + \frac{\overline{W}}{R} - \frac{1}{2} \left(\frac{\partial \overline{W}}{\partial Y} \right)^2 - \frac{\partial \overline{W}}{\partial Y} \frac{\partial \overline{W}^*}{\partial Y} - \left(A_{12}^* \overline{N}_x^{\mathrm{T}} + A_{22}^* \overline{N}_y^{\mathrm{T}} \right) \right] \mathrm{d}Y = 0 \tag{18b}$$

Because of Eq. (18), the in-plane boundary condition $\overline{V}=0$ (at $X=0$, L) is not needed in Eq. (17). The average end-shortening relationship is defined as

$$\begin{aligned}\frac{\Delta_x}{L} &= -\frac{1}{2\pi RL}\int_0^{2\pi R}\int_0^L \frac{\partial \overline{U}}{\partial X}\,\mathrm{d}X\,\mathrm{d}Y \\ &= -\frac{1}{2\pi RL}\int_0^{2\pi R}\int_0^L \left[\left(A_{11}^*\frac{\partial^2\overline{F}}{\partial Y^2}+A_{12}^*\frac{\partial^2\overline{F}}{\partial X^2}\right)+\left(B_{11}^*-\frac{4}{3t^2}E_{11}^*\right)\frac{\partial\overline{\Psi}_x}{\partial X}+\left(B_{12}^*-\frac{4}{3t^2}E_{12}^*\right)\frac{\partial\overline{\Psi}_y}{\partial Y}\right. \\ &\quad \left.-\frac{4}{3t^2}\left(E_{11}^*\frac{\partial^2\overline{W}}{\partial X^2}+E_{12}^*\frac{\partial^2\overline{W}}{\partial Y^2}\right)-\frac{1}{2}\left(\frac{\partial\overline{W}}{\partial X}\right)^2-\frac{\partial\overline{W}}{\partial X}\frac{\partial\overline{W}^*}{\partial X}-\left(A_{11}^*\overline{N}_x^{\mathrm{T}}+A_{12}^*\overline{N}_y^{\mathrm{T}}\right)\right]\mathrm{d}X\,\mathrm{d}Y\end{aligned} \tag{19}$$

In the above equations and what follows, the reduced stiffness matrices $[A_{ij}^*]$, $[B_{ij}^*]$, $[D_{ij}^*]$, $[E_{ij}^*]$, $[F_{ij}^*]$ and $[H_{ij}^*]$ (i, $j=1$, 2, 6) are functions of temperature and position, determined through relationships (Shen and Li, 2002)

$$\begin{aligned}&\mathbf{A}^*=\mathbf{A}^{-1},\quad \mathbf{B}^*=-\mathbf{A}^{-1}\mathbf{B},\quad \mathbf{D}^*=\mathbf{D}-\mathbf{B}\mathbf{A}^{-1}\mathbf{B},\quad \mathbf{E}^*=-\mathbf{A}^{-1}\mathbf{E},\quad \mathbf{F}^*=\mathbf{F}-\mathbf{E}\mathbf{A}^{-1}\mathbf{B},\\ &\mathbf{H}^*=\mathbf{H}-\mathbf{E}\mathbf{A}^{-1}\mathbf{E}\end{aligned} \tag{20}$$

where A_{ij},B_{ij} etc., are the shell stiffnesses, defined in the standard way (Reddy and Liu, 1985).

3. Analytical method and asymptotic solutions

Having developed the theory, we are now in a position to solve Eqs. (10)–(13) with boundary condition (17). Before proceeding, it is convenient first to define the following dimensionless quantities (with γ_{ijk} in Eqs. (28) and (29) below are defined as in Shen and Li (2002))

$$\begin{aligned}&x=\pi X/L, y=Y/R, \beta=L/\pi R, \overline{Z}=L^2/Rt,\quad \varepsilon=(\pi^2R/L^2)[D_{11}^*D_{22}^*A_{11}^*A_{22}^*]^{1/4}\\ &(W,W^*)=\varepsilon(\overline{W},\overline{W}^*)/[D_{11}^*D_{22}^*A_{11}^*A_{22}^*]^{1/4},\quad F=\varepsilon^2\overline{F}/[D_{11}^*D_{22}^*]^{1/2}\\ &(\Psi_x,\Psi_y)=\varepsilon^2(\overline{\Psi}_x,\overline{\Psi}_y)(L/\pi)/[D_{11}^*D_{22}^*A_{11}^*A_{22}^*]^{1/4},\quad \gamma_{12}=(D_{12}^*+2D_{66}^*)D_{11}^*\\ &\gamma_{22}=(A_{12}^*+A_{66}^*/2)/A_{22}^*,\quad \gamma_{14}=[D_{22}^*/D_{11}^*]^{1/2},\quad \gamma_{24}=[A_{11}^*/A_{22}^*]^{1/2},\quad \gamma_5=-A_{12}^*/A_{22}^*\\ &(\gamma_{31},\gamma_{41})=(L^2/\pi^2)(A_{55}-8D_{55}/t^2+16F_{55}/t^4, A_{44}-8D_{44}/t^2+16F_{44}/t^4)/D_{11}^*\\ &(\gamma_{T1},\gamma_{T2})=(A_x^{\mathrm{T}},A_y^{\mathrm{T}})R[A_{11}^*A_{22}^*/D_{11}^*D_{22}^*]^{1/4}\\ &(M_x,P_x)=\varepsilon^2(\overline{M}_x,4\overline{P}_x/3t^2)(L^2/\pi^2)/D_{11}^*[D_{11}^*D_{22}^*A_{11}^*A_{22}^*]^{1/4}\\ &\lambda_p=\sigma_x/(2/Rt)[D_{11}^*D_{22}^*/A_{11}^*A_{22}^*]^{1/4},\quad \lambda_q=q(3)^{3/4}LR^{3/2}[A_{11}^*A_{22}^*]^{1/8}/4\pi[D_{11}^*D_{22}^*]^{3/8}\\ &\delta_p=(\Delta_x/L)/(2/R)[D_{11}^*D_{22}^*A_{11}^*A_{22}^*]^{1/4},\quad \delta_q=(\Delta_x/L)(3)^{3/4}LR^{1/2}/4\pi[D_{11}^*D_{22}^*A_{11}^*A_{22}^*]^{3/8}\end{aligned} \tag{21}$$

in which $A_x^{\mathrm{T}}=A_y^{\mathrm{T}}$ are defined by

$$\begin{bmatrix}A_x^{\mathrm{T}}\\ A_y^{\mathrm{T}}\end{bmatrix}T_1=-\int_{-t/2}^{t/2}\begin{bmatrix}A_x\\ A_y\end{bmatrix}T(Z)\,\mathrm{d}Z \tag{22}$$

where $T_1=(T_{\mathrm{U}}+T_{\mathrm{L}}-2T_0)/2$, and the details of A_x^{T} can be found in Appendix A.

The nonlinear Eqs. (10)–(13) may then be written in dimensionless form as

$$\varepsilon^2L_{11}(W)-\varepsilon L_{12}(\Psi_x)-\varepsilon L_{13}(\Psi_y)+\varepsilon\gamma_{14}L_{14}(F)-\gamma_{14}F_{,xx}=\gamma_{14}\beta^2L(W+W^*,F)+\gamma_{14}\frac{4}{3}(3)^{1/4}\lambda_q\varepsilon^{3/2} \tag{23}$$

$$L_{21}(F)+\gamma_{24}L_{22}(\Psi_x)+\gamma_{24}L_{23}(\Psi_y)-\varepsilon\gamma_{24}L_{24}(W)+\gamma_{24}W_{,xx}=-\frac{1}{2}\gamma_{24}\beta^2L(W+2W^*,W) \tag{24}$$

$$\varepsilon L_{31}(W)+L_{32}(\Psi_x)-L_{33}(\Psi_y)+\gamma_{14}L_{34}(F)=0 \tag{25}$$

$$\varepsilon L_{41}(W)-L_{42}(\Psi_x)+L_{43}(\Psi_y)+\gamma_{14}L_{44}(F)=0 \tag{26}$$

where all the dimensionless operators $L_{ij}(\ )$ and $L(\ )$ are defined as in Shen and Li (2002).

For most FGMs $[D_{11}^*D_{22}^*A_{11}^*A_{22}^*]^{1/4}\cong 0.3t$. Moreover, when $\overline{Z}=(L^2/Rt)>2.96$, then from Eq. (21) $\varepsilon<1$. In particular, for homogeneous isotropic cylindrical shells, $\varepsilon=\pi^2/\overline{Z}_B\sqrt{12}$, where $\overline{Z}_B=(L^2/Rt)[1-\nu^2]^{1/2}$ is the Batdorf shell parameter, which should be greater than 2.85 in the case of classical linear buckling analysis (Batdorf, 1947). In practice, the shell structure will have $\overline{Z}\geqslant 10$, so that we always have $\varepsilon\ll 1$. When $\varepsilon<1$, Eqs. (23)–(26) are of the boundary layer type, from which nonlinear prebuckling deformations, large deflections in the postbuckling range, and initial geometric imperfections of the shell, can be considered simultaneously.

The boundary conditions of Eq. (17) become

$$W=\Psi_y=0,\quad M_x=P_x=0\quad\text{(simply supported)} \tag{27a}$$

$$W=\Psi_x=\Psi_y\quad\text{(clamped)} \tag{27b}$$

$$\frac{1}{2\pi}\int_0^{2\pi}\beta^2\frac{\partial^2F}{\partial y^2}\,\mathrm{d}y+2\lambda_p\varepsilon+\frac{2}{3}(3)^{1/4}\lambda_q\varepsilon^{3/2}a=0 \tag{27c}$$

and the closed condition becomes

$$\int_0^{2\pi}\left[\left(\frac{\partial^2F}{\partial x^2}-\gamma_5\beta^2\frac{\partial^2F}{\partial y^2}\right)+\gamma_{24}\left(\gamma_{220}\frac{\partial\Psi_x}{\partial x}+\gamma_{522}\beta\frac{\partial\Psi_y}{\partial y}\right)-\varepsilon\gamma_{24}\left(\gamma_{240}\frac{\partial^2W}{\partial x^2}+\gamma_{622}\beta^2\frac{\partial^2W}{\partial y^2}\right)+\gamma_{24}W\right.$$
$$\left.-\frac{1}{2}\gamma_{24}\beta^2\left(\frac{\partial W}{\partial y}\right)^2-\gamma_{24}\beta^2\frac{\partial W}{\partial y}\frac{\partial W^*}{\partial y}+\varepsilon(\gamma_{T2}-\gamma_5\gamma_{T1})T_1\right]\mathrm{d}y=0 \tag{28}$$

In this section two loading conditions will be considered, so that the unit end-shortening relationship may be written in two dimensionless forms as

$$\delta_q=-\frac{(3)^{3/4}}{8\pi^2\gamma_{24}}\varepsilon^{-3/2}\int_0^{2\pi}\int_0^{\pi}\left[\left(\gamma_{24}^2\beta^2\frac{\partial^2F}{\partial y^2}-\gamma_5\frac{\partial^2F}{\partial x^2}\right)+\gamma_{24}\left(\gamma_{511}\frac{\partial\Psi_x}{\partial x}+\gamma_{233}\beta\frac{\partial\Psi_y}{\partial y}\right)\right.$$
$$\left.-\varepsilon\gamma_{24}\left(\gamma_{611}\frac{\partial^2W}{\partial x^2}+\gamma_{244}\beta^2\frac{\partial^2W}{\partial y^2}\right)-\frac{1}{2}\gamma_{24}\left(\frac{\partial W}{\partial x}\right)^2-\gamma_{24}\frac{\partial W}{\partial x}\frac{\partial W^*}{\partial x}+\varepsilon(\gamma_{24}^2\gamma_{T1}-\gamma_5\gamma_{T2})T_1\right]\mathrm{d}x\,\mathrm{d}y \tag{29a}$$

$$\delta_p=-\frac{1}{4\pi^2\gamma_{24}}\varepsilon^{-1}\int_0^{2\pi}\int_0^{\pi}\left[\left(\gamma_{24}^2\beta^2\frac{\partial^2F}{\partial y^2}-\gamma_5\frac{\partial^2F}{\partial x^2}\right)+\gamma_{24}\left(\gamma_{511}\frac{\partial\Psi_x}{\partial x}+\gamma_{233}\beta\frac{\partial\Psi_y}{\partial y}\right)\right.$$
$$\left.-\varepsilon\gamma_{24}\left(\gamma_{611}\frac{\partial^2W}{\partial x^2}+\gamma_{244}\beta^2\frac{\partial^2W}{\partial y^2}\right)-\frac{1}{2}\gamma_{24}\left(\frac{\partial W}{\partial x}\right)^2-\gamma_{24}\frac{\partial W}{\partial x}\frac{\partial W^*}{\partial x}+\varepsilon(\gamma_{24}^2\gamma_{T1}-\gamma_5\gamma_{T2})T_1\right]\mathrm{d}x\,\mathrm{d}y \tag{29b}$$

By virtue of the fact that T_1 is assumed to be uniform, the thermal coupling in Eqs. (10)–(13) vanishes, but terms in T_1 intervene in Eqs. (28) and (29).

Applying Eqs. (23)–(19), the postbuckling behavior of perfect and imperfect FGM cylindrical shells subjected to combined axial and radial loads in thermal environments is determined by means of a singular perturbation technique. The essence of this procedure, in the present case, is to assume that

$$
\begin{aligned}
W &= w(x,y,\varepsilon) + \widetilde{W}(x,\xi,y,\varepsilon) + \widehat{W}(x,\zeta,y,\varepsilon)\\
F &= f(x,y,\varepsilon) + \widetilde{F}(x,\xi,y,\varepsilon) + \widehat{F}(x,\zeta,y,\varepsilon)\\
\Psi_x &= \psi_x(x,y,\varepsilon) + \widetilde{\Psi}_x(x,\xi,y,\varepsilon) + \widehat{\Psi}_x(x,\zeta,y,\varepsilon)\\
\Psi_y &= \psi_y(x,y,\varepsilon) + \widetilde{\Psi}_y(x,\xi,y,\varepsilon) + \widehat{\Psi}_y(x,\zeta,y,\varepsilon)
\end{aligned}
\tag{30}
$$

where ε is a small perturbation parameter (provided $\overline{Z} > 2.96$) as defined in Eq. (21) and $w(x,y,\varepsilon)$, $f(x,y,\varepsilon)$, $\psi_x(x,y,\varepsilon)$, and $\psi_y(x,y,\varepsilon)$ are called the outer or regular solutions of the shell. $\widetilde{W}(x,\xi,y,\varepsilon)$, $\widetilde{F}(x,\xi,y,\varepsilon)$, $\widetilde{\Psi}_x(x,\xi,y,\varepsilon)$, $\widetilde{\Psi}_y(x,\xi,y,\varepsilon)$ and $\widehat{W}(x,\zeta,y,\varepsilon)$, $\widehat{F}(x,\zeta,y,\varepsilon)$, $\widehat{\Psi}_x(x,\zeta,y,\varepsilon)$, $\widehat{\Psi}_y(x,\zeta,y,\varepsilon)$ are the boundary layer solutions near the $x=0$ and $x=\pi$ edges, respectively, and ξ and ζ are the boundary layer variables, defined as

$$
\xi = x/\sqrt{\varepsilon}, \quad \zeta = (\pi - x)/\sqrt{\varepsilon} \tag{31}
$$

This means that for homogeneous isotropic cylindrical shells, the width of the boundary layers is of order $\sqrt{Rt}$. In Eq. (30) the regular and boundary layer solutions are taken in the forms of perturbation expansions as

$$
\begin{aligned}
w(x,y,\varepsilon) &= \sum_{j=1} \varepsilon^{j/2} w_{j/2}(x,y), \quad f(x,y,\varepsilon) = \sum_{j=0} \varepsilon^{j/2} f_{j/2}(x,y)\\
\psi_x(x,y,\varepsilon) &= \sum_{j=1} \varepsilon^{j/2} (\psi_x)_{j/2}(x,y), \quad \psi_y(x,y,\varepsilon) = \sum_{j=1} \varepsilon^{j/2} (\psi_y)_{j/2}(x,y)
\end{aligned}
\tag{32a}
$$

$$
\begin{aligned}
\widetilde{W}(x,\xi,y,\varepsilon) &= \sum_{j=0} \varepsilon^{j/2+1} \widetilde{W}_{j/2+1}(x,\xi,y), \quad \widetilde{F}(x,\xi,y,\varepsilon) = \sum_{j=0} \varepsilon^{j/2+2} \widetilde{F}_{j/2+2}(x,\xi,y)\\
\widetilde{\Psi}_x(x,\xi,y,\varepsilon) &= \sum_{j=0} \varepsilon^{(j+3)/2} (\widetilde{\Psi}_x)_{(j+3)/2}(x,\xi,y), \quad \widetilde{\Psi}_y(x,\xi,y,\varepsilon) = \sum_{j=0} \varepsilon^{j/2+2} (\widetilde{\Psi}_y)_{j/2+2}(x,\xi,y)
\end{aligned}
\tag{32b}
$$

$$
\begin{aligned}
\widehat{W}(x,\zeta,y,\varepsilon) &= \sum_{j=0} \varepsilon^{j/2+1} \widehat{W}_{j/2+1}(x,\zeta,y), \quad \widehat{F}(x,\zeta,y,\varepsilon) = \sum_{j=0} \varepsilon^{j/2+2} \widehat{F}_{j/2+2}(x,\zeta,y)\\
\widehat{\Psi}_x(x,\zeta,y,\varepsilon) &= \sum_{j=0} \varepsilon^{(j+3)/2} (\widehat{\Psi}_x)_{(j+3)/2}(x,\zeta,y), \quad \widehat{\Psi}_y(x,\zeta,y,\varepsilon) = \sum_{j=0} \varepsilon^{j/2+2} (\widehat{\Psi}_y)_{j/2+2}(x,\zeta,y)
\end{aligned}
\tag{32c}
$$

The initial buckling mode is assumed to have the form

$$
w_2(x,y) = A_{11}^{(2)} \sin mx \sin ny \tag{33}
$$

and the initial geometric imperfection is assumed to have a similar form

$$
W^*(x,y,\varepsilon) = \varepsilon^2 a_{11}^* \sin mx \sin ny = \varepsilon^2 \mu A_{11}^{(2)} \sin mx \sin ny \tag{34}
$$

where $\mu = a_{11}^*/A_{11}^{(2)}$ is the imperfection parameter.

Substituting Eqs. (30)–(32) into Eqs. (23)–(26), collecting the terms of the same order of ε, three sets of perturbation equations are obtained for the regular and boundary layer solutions, respectively. It has been shown (Shen and Chen, 1988, 1990) that the effect of the boundary layer on the buckling load of the shell under axial compression is quite different from that of the shell subjected to external pressure. To this end, two kinds of loading conditions will be considered.

Case (1): high values of external pressure combined with relatively low axial load. Let

$$
\frac{P}{\pi R^2 q} = b_1 \tag{35a}
$$

or

$$\frac{2\lambda_p\varepsilon}{\frac{4}{3}(3)^{1/4}\lambda_q\varepsilon^{3/2}}=\frac{b_1}{2} \tag{35b}$$

In this case, the boundary condition of Eq. (27c) becomes

$$\frac{1}{2\pi}\int_0^{2\pi}\beta^2\frac{\partial^2 F}{\partial y^2}\,\mathrm{d}y+\frac{2}{3}(3)^{1/4}\lambda_q\varepsilon^{3/2}(a+b_1)=0 \tag{36}$$

For convenience we replace $(a+b_1)$ with a_1 in Eq. (38) below, by using Eqs. (33) and (34) to solve these perturbation equations of each order, and matching the regular solutions with the boundary layer solutions at the each end of the shell, so that the asymptotic solutions satisfying the clamped boundary conditions are constructed as

$$\begin{aligned}W=\varepsilon^{3/2}&\left[A_{00}^{(3/2)}-A_{00}^{(3/2)}\left(a_{01}^{(3/2)}\cos\phi\frac{x}{\sqrt{\varepsilon}}+a_{10}^{(3/2)}\sin\phi\frac{x}{\sqrt{\varepsilon}}\right)\exp\left(-\vartheta\frac{x}{\sqrt{\varepsilon}}\right)\right.\\&\left.-A_{00}^{(3/2)}\left(a_{01}^{(3/2)}\cos\phi\frac{\pi-x}{\sqrt{\varepsilon}}+a_{10}^{(3/2)}\sin\phi\frac{\pi-x}{\sqrt{\varepsilon}}\right)\exp\left(-\vartheta\frac{\pi-x}{\sqrt{\varepsilon}}\right)\right]+\varepsilon^2\left[A_{11}^{(2)}\sin mx\sin ny\right]\\&+\varepsilon^3\left[A_{11}^{(3)}\sin mx\sin ny\right]+\varepsilon^4\left[A_{00}^{(4)}+A_{11}^{(4)}\sin mx\sin ny+A_{20}^{(4)}\cos 2mx+A_{02}^{(4)}\cos 2ny\right]+\mathrm{O}(\varepsilon^5)\end{aligned} \tag{37}$$

$$\begin{aligned}F=&-\frac{1}{2}B_{00}^{(0)}\left(\beta^2x^2+a_1\frac{y^2}{2}\right)+\varepsilon\left[-\frac{1}{2}B_{00}^{(1)}\left(\beta^2x^2+a_1\frac{y^2}{2}\right)\right]+\varepsilon^2\left[-\frac{1}{2}B_{00}^{(2)}\left(\beta^2x^2+a_1\frac{y^2}{2}\right)+B_{11}^{(2)}\sin mx\sin ny\right]\\&+\varepsilon^{5/2}\left[A_{00}^{(3/2)}\left(b_{01}^{(5/2)}\cos\phi\frac{x}{\sqrt{\varepsilon}}+b_{10}^{(5/2)}\sin\phi\frac{x}{\sqrt{\varepsilon}}\right)\exp\left(-\vartheta\frac{x}{\sqrt{\varepsilon}}\right)\right.\\&\left.+A_{00}^{(3/2)}\left(b_{01}^{(5/2)}\cos\phi\frac{\pi-x}{\sqrt{\varepsilon}}+b_{10}^{(5/2)}\sin\phi\frac{\pi-x}{\sqrt{\varepsilon}}\right)\exp\left(-\vartheta\frac{\pi-x}{\sqrt{\varepsilon}}\right)\right]+\varepsilon^3\left[-\frac{1}{2}B_{00}^{(3)}\left(\beta^2x^2+a_1\frac{y^2}{2}\right)\right]\\&+\varepsilon^4\left[-\frac{1}{2}B_{00}^{(4)}\left(\beta^2x^2+a_1\frac{y^2}{2}\right)+B_{20}^{(4)}\cos 2mx+B_{02}^{(4)}\cos 2ny\right]+\mathrm{O}(\varepsilon^5)\end{aligned} \tag{38}$$

$$\begin{aligned}\Psi_x=\varepsilon^2&\left[C_{11}^{(2)}\cos mx\sin ny+\left(c_{01}^{(2)}\cos\phi\frac{x}{\sqrt{\varepsilon}}+c_{10}^{(2)}\sin\phi\frac{x}{\sqrt{\varepsilon}}\right)\exp\left(-\vartheta\frac{x}{\sqrt{\varepsilon}}\right)\right.\\&\left.+\left(c_{01}^{(2)}\cos\phi\frac{\pi-x}{\sqrt{\varepsilon}}+c_{10}^{(2)}\sin\phi\frac{\pi-x}{\sqrt{\varepsilon}}\right)\exp\left(-\vartheta\frac{\pi-x}{\sqrt{\varepsilon}}\right)\right]+\varepsilon^3[C_{11}^{(3)}\cos mx\sin ny]\\&+\varepsilon^4[C_{11}^{(4)}\cos mx\sin ny+C_{20}^{(4)}\sin 2mx]+\mathrm{O}(\varepsilon^5)\end{aligned} \tag{39}$$

$$\Psi_y=\varepsilon^2\left[D_{11}^{(2)}\sin mx\cos ny\right]+\varepsilon^3\left[D_{11}^{(3)}\sin mx\cos ny\right]+\varepsilon^4\left[D_{11}^{(4)}\sin mx\cos ny+D_{02}^{(4)}\sin 2ny\right]+\mathrm{O}(\varepsilon^5) \tag{40}$$

Note that, because of Eq. (37), the prebuckling deformation of the shell is nonlinear, and all of the coefficients in Eqs. (37)–(40) are related and can be expressed in terms of $A_{11}^{(2)}$, but for the sake of brevity the detailed expressions are not shown, whereas ϑ and ϕ are given in detail in Appendix A.

Next, upon substitution of Eqs. (37)–(40) into the boundary condition (36) and into Eq. (29a), the postbuckling equilibrium paths can be written as

$$\lambda_q=\frac{1}{4}(3)^{3/4}\varepsilon^{-3/2}\left[\lambda_q^{(0)}+\lambda_q^{(2)}(A_{11}^{(2)}\varepsilon^2)^2+\cdots\right] \tag{41}$$

and

$$\delta_q = \delta_q^{(0)} - \delta_q^{(T)} + \delta_q^{(2)}\left(A_{11}^{(2)}\varepsilon^2\right)^2 + \cdots \tag{42}$$

In Eqs. (41) and (42), $(A_{11}^{(2)}\varepsilon^2)$ is taken as the second perturbation parameter relating to the dimensionless maximum deflection. If the maximum deflection is assumed to be at the point $(x,y) = (\pi/2m,\pi/2n)$, then

$$A_{11}^{(2)}\varepsilon^2 = W_{\mathrm{m}} - \Theta_1 W_{\mathrm{m}}^2 + \cdots \tag{43a}$$

where W_{m} is the dimensionless form of the maximum deflection of the shell that can be written as

$$W_{\mathrm{m}} = \frac{1}{C_3}\left[\varepsilon\frac{t}{[D_{11}^* D_{22}^* A_{11}^* A_{22}^*]^{1/4}}\frac{\overline{W}}{t} + \Theta_2\right] \tag{43b}$$

All symbols used in Eqs. (41)–(43) and Eqs. (50)–(52) below are also described in detail in Appendix A.

Case (2): high values of axial compression combined with relatively low external pressure. Let

$$\frac{\pi R^2 q}{P} = b_2 \tag{44a}$$

or

$$\frac{\frac{4}{3}(3)^{1/4}\lambda_q\varepsilon^{3/2}}{2\lambda_p\varepsilon} = 2b_2 \tag{44b}$$

In this case, the boundary condition of Eq. (27c) becomes

$$\frac{1}{2\pi}\int_0^{2\pi}\beta^2\frac{\partial^2 F}{\partial y^2}\,\mathrm{d}y + 2\lambda_p\varepsilon(1+ab_2) = 0 \tag{45}$$

Similarly, by taking $a_2 = 2b_2/(1+ab_2)$ and using a singular perturbation procedure, the asymptotic solutions satisfying the clamped boundary conditions are obtained as

$$\begin{aligned} W = {} & \varepsilon\left[A_{00}^{(1)} - A_{00}^{(1)}\left(a_{01}^{(1)}\cos\phi\frac{x}{\sqrt{\varepsilon}} + a_{10}^{(1)}\sin\phi\frac{x}{\sqrt{\varepsilon}}\right)\exp\left(-\vartheta\frac{x}{\sqrt{\varepsilon}}\right)\right. \\ & \left. - A_{00}^{(1)}\left(a_{01}^{(1)}\cos\phi\frac{\pi-x}{\sqrt{\varepsilon}} + a_{10}^{(1)}\sin\phi\frac{\pi-x}{\sqrt{\varepsilon}}\right)\exp\left(-\vartheta\frac{\pi-x}{\sqrt{\varepsilon}}\right)\right] \\ & + \varepsilon^2\left[A_{11}^{(2)}\sin mx\sin ny + A_{02}^{(2)}\cos 2ny - (A_{02}^{(2)}\cos 2ny)\left(a_{01}^{(1)}\cos\phi\frac{x}{\sqrt{\varepsilon}} + a_{10}^{(1)}\sin\phi\frac{x}{\sqrt{\varepsilon}}\right)\exp\left(-\vartheta\frac{x}{\sqrt{\varepsilon}}\right)\right. \\ & \left. - (A_{02}^{(2)}\cos 2ny)\left(a_{01}^{(1)}\cos\phi\frac{\pi-x}{\sqrt{\varepsilon}} + a_{10}^{(1)}\sin\phi\frac{\pi-x}{\sqrt{\varepsilon}}\right)\exp\left(-\vartheta\frac{\pi-x}{\sqrt{\varepsilon}}\right)\right] \\ & + \varepsilon^3\left[A_{11}^{(3)}\sin mx\sin ny + A_{02}^{(3)}\cos 2ny\right] + \varepsilon^4\left[A_{00}^{(4)} + A_{11}^{(4)}\sin mx\sin ny + A_{20}^{(4)}\cos 2mx + A_{02}^{(4)}\cos 2ny\right. \\ & \left. + A_{13}^{(4)}\sin mx\sin 3ny + A_{04}^{(4)}\cos 4ny\right] + \mathrm{O}(\varepsilon^5) \end{aligned} \tag{46}$$

$$\begin{aligned} F = {} & -\frac{1}{2}B_{00}^{(0)}(a_2\beta^2x^2 + y^2) + \varepsilon\left[-\frac{1}{2}B_{00}^{(1)}(a_2\beta^2x^2 + y^2)\right] + \varepsilon^2\left[-\frac{1}{2}B_{00}^{(2)}(a_2\beta^2x^2 + y^2) + B_{11}^{(2)}\sin mx\sin ny\right. \\ & + A_{00}^{(1)}\left(b_{01}^{(2)}\cos\phi\frac{x}{\sqrt{\varepsilon}} + b_{10}^{(2)}\sin\phi\frac{x}{\sqrt{\varepsilon}}\right)\exp\left(-\vartheta\frac{x}{\sqrt{\varepsilon}}\right) \\ & \left. + A_{00}^{(1)}\left(b_{01}^{(2)}\cos\phi\frac{\pi-x}{\sqrt{\varepsilon}} + b_{10}^{(2)}\sin\phi\frac{\pi-x}{\sqrt{\varepsilon}}\right)\exp\left(-\vartheta\frac{\pi-x}{\sqrt{\varepsilon}}\right)\right] \end{aligned}$$

$$+\varepsilon^3\left[-\frac{1}{2}B_{00}^{(3)}(a_2\beta^2x^2+y^2)+B_{02}^{(3)}\cos 2ny+(A_{02}^{(2)}\cos 2ny)\left(b_{01}^{(3)}\cos\phi\frac{x}{\sqrt{\varepsilon}}+b_{10}^{(3)}\sin\phi\frac{x}{\sqrt{\varepsilon}}\right)\exp\left(-\vartheta\frac{x}{\sqrt{\varepsilon}}\right)\right.$$
$$\left.+(A_{02}^{(2)}\cos 2ny)\left(b_{01}^{(3)}\cos\phi\frac{\pi-x}{\sqrt{\varepsilon}}+b_{10}^{(3)}\sin\phi\frac{\pi-x}{\sqrt{\varepsilon}}\right)\exp\left(-\vartheta\frac{\pi-x}{\sqrt{\varepsilon}}\right)\right]$$
$$+\varepsilon^4\left[-\frac{1}{2}B_{00}^{(4)}(a_2\beta^2x^2+y^2)+B_{20}^{(4)}\cos 2mx+B_{02}^{(4)}\cos 2ny+B_{13}^{(4)}\sin mx\sin 3ny\right]+\mathrm{O}(\varepsilon^5) \tag{47}$$

$$\Psi_x=\varepsilon^{3/2}\left[A_{00}^{(1)}c_{10}^{(3/2)}\sin\phi\frac{x}{\sqrt{\varepsilon}}\exp\left(-\vartheta\frac{x}{\sqrt{\varepsilon}}\right)+A_{00}^{(1)}c_{10}^{(3/2)}\sin\phi\frac{\pi-x}{\sqrt{\varepsilon}}\exp\left(-\vartheta\frac{\pi-x}{\sqrt{\varepsilon}}\right)\right]+\varepsilon^2[C_{11}^{(2)}\cos mx\sin ny]$$
$$+\varepsilon^{5/2}\left[(A_{02}^{(2)}\cos 2ny)c_{10}^{(5/2)}\sin\phi\frac{x}{\sqrt{\varepsilon}}\exp\left(-\vartheta\frac{x}{\sqrt{\varepsilon}}\right)+(A_{02}^{(2)}\cos 2ny)c_{10}^{(5/2)}\sin\phi\frac{\pi-x}{\sqrt{\varepsilon}}\exp\left(-\vartheta\frac{\pi-x}{\sqrt{\varepsilon}}\right)\right]$$
$$+\varepsilon^3[C_{11}^{(3)}\cos mx\sin ny]+\varepsilon^4\left[C_{11}^{(4)}\cos mx\sin ny+C_{20}^{(4)}\sin 2mx+C_{13}^{(4)}\cos mx\sin 3ny\right]+\mathrm{O}(\varepsilon^5) \tag{48}$$

$$\Psi_y=\varepsilon^2\left[D_{11}^{(2)}\sin mx\cos ny\right]+\varepsilon^3\left[D_{11}^{(3)}\sin mx\cos ny+D_{02}^{(3)}\sin 2ny\right.$$
$$-\left(A_{02}^{(2)}2n\beta\sin 2ny\right)\left(d_{01}^{(3)}\cos\phi\frac{x}{\sqrt{\varepsilon}}+d_{10}^{(3)}\sin\phi\frac{x}{\sqrt{\varepsilon}}\right)\exp\left(-\vartheta\frac{x}{\sqrt{\varepsilon}}\right)$$
$$\left.-\left(A_{02}^{(2)}2n\beta\sin 2ny\right)\left(d_{01}^{(3)}\cos\phi\frac{\pi-x}{\sqrt{\varepsilon}}+d_{10}^{(3)}\sin\phi\frac{\pi-x}{\sqrt{\varepsilon}}\right)\exp\left(-\vartheta\frac{\pi-x}{\sqrt{\varepsilon}}\right)\right]$$
$$+\varepsilon^4\left[D_{11}^{(4)}\sin mx\cos ny+D_{02}^{(4)}\sin 2ny+D_{13}^{(4)}\sin mx\cos 3ny\right]+\mathrm{O}(\varepsilon^5) \tag{49}$$

Next, upon substitution of Eqs. (46)–(49) into the boundary condition (45) and into Eq. (29b), the post-buckling equilibrium paths can be written as

$$\lambda_p=\frac{1}{1+ab_2}[\lambda_p^{(0)}-\lambda_p^{(2)}(A_{11}^{(2)}\varepsilon)^2+\lambda_p^{(4)}(A_{11}^{(2)}\varepsilon)^4+\cdots] \tag{50}$$

and

$$\delta_p=\delta_p^{(0)}-\delta_p^{(T)}+\delta_p^{(2)}(A_{11}^{(2)}\varepsilon)^2+\delta_p^{(4)}(A_{11}^{(2)}\varepsilon)^4+\cdots \tag{51}$$

In Eqs. (50) and (51), similarly, $(A_{11}^{(2)}\varepsilon)$ is taken as the second perturbation parameter in this case, and we have

$$A_{11}^{(2)}\varepsilon=W_{\mathrm{m}}-\Theta_3W_{\mathrm{m}}^2+\cdots \tag{52a}$$

and the dimensionless maximum deflection of the shell is written as

$$W_{\mathrm{m}}=\frac{1}{C_3}\left[\frac{t}{[D_{11}^*D_{22}^*A_{11}^*A_{22}^*]^{1/4}}\frac{\overline{W}}{t}+\Theta_4\right] \tag{52b}$$

Eqs. (41)–(43) and (50)–(52) can be employed to obtain numerical results for full nonlinear postbuckling load-shortening or load–deflection curves of FGM cylindrical shells subjected to combined axial and radial loads in thermal environments. Buckling under external pressure and buckling under axial compression follow as two limiting cases. By increasing b_1 and b_2 respectively, the interaction curve of an FGM

cylindrical shell under combined loading can be constructed with these two lines. Note that since $b_2 = 1/b_1$ only one load-proportional parameter should be determined in advance. The initial buckling load of a perfect shell can readily be obtained numerically, by setting $\overline{W}^*/t = 0$ (or $\mu = 0$), while taking $\overline{W}/t = 0$ (note that $W_m \neq 0$). In this case, the minimum buckling load is determined by considering Eq. (41) or (50) for various values of the buckling mode (m, n), which determine the number of half-waves in the X-direction and of full waves in the Y-direction.

4. Numerical results and discussions

Numerical results are presented in this section for FGM cylindrical shells with two constituent materials. Two sets of material mixture are considered. One is silicon nitride and stainless steel, referred to as Si_3N_4/SUS304, and the other is zirconium oxide and titanium alloy, referred to as ZrO_2/Ti–6Al–4V. However, the analysis is equally applicable to other types of FGMs as well. Typical values for Young's modulus E (in Pa), thermal expansion coefficient α (in K^{-1}) and the thermal conductivity κ (in W/m K) of these materials are listed in Table 1 (from Reddy and Chin, 1998). Poisson's ratio ν is assumed to be a constant, and $\nu = 0.28$.

The accuracy and effectiveness of the present method for the buckling and postbuckling analysis of isotropic or multilayered cylindrical shells subjected to combined loading of external pressure and axial compression were examined by many comparison studies given in Shen and Chen (1991), Shen et al. (1993), and Shen (1997, 2001). In addition, the buckling hoop stresses for isotropic thin cylindrical shells subjected to

Table 1
Temperature-dependent coefficients for ceramics and metals, from Reddy and Chin (1998)

Materials		P_0	P_{-1}	P_1	P_2	P_3
Zirconia	E	244.27e+9	0	−1.371e−3	1.214e−6	−3.681e−10
	α	12.766e−6	0	−1.491e−3	1.006e−5	−6.778e−11
	κ	1.7000	–	–	–	–
Silicon nitride	E	348.43e+9	0	−3.070e−4	2.160e−7	−8.946e−11
	α	5.8723e−6	0	9.095e−4	0	0
	κ	13.723	–	–	–	–
Ti–6Al–4V	E	122.56e+9	0	−4.586e−4	0	0
	α	7.5788e−6	0	6.638e−4	−3.147e−6	0
	κ	1.0000	–	–	–	–
Stainless steel	E	201.04e+9	0	3.079e−4	−6.534e−7	0
	α	12.330e−6	0	8.086e−4	0	0
	κ	15.379	–	–	–	–

Table 2
Comparisons of buckling stresses $(\sigma_y)_{cr}$ (in N/mm^2) for perfect isotropic thin cylindrical shells subjected to combined axial and radial loads ($R = 254$ mm, $E = 204$ kN/mm^2, $\nu = 0.3$)

L/R	R/t	b_1	Present	Galletly et al. (1987)
0.418	304	8	53.706 (15)	58.3 (15)
0.415	308	4	70.531 (16)	78.8 (16)
0.418	304	1.05	92.377 (16)	97.2 (17)
0.415	304	0	103.116 (17)	108.0 (17)

combined axial and radial loads are calculated and compared in Table 2 with the results obtained by Galletly et al. (1987) based on the classical shell theory, in which $(\sigma_y)_{cr}$ is defined by $q_{cr}(R/t)$. The material properties adopted are $E = 204$ kN/mm^2 and $v = 0.3$. It can be seen that the present results agree well but slightly lower than those of Galletly et al. (1987).

The buckling loads (σ_{cr},q_{cr}) (in MPa) for perfect Si_3N_4/SUS304 and ZrO_2/Ti–6Al–4V thin and moderately thick cylindrical shells under four sets of combined loading conditions, i.e. lateral pressure alone ($b_1 = 0$), combined loading case (1) ($b_1 = 10$), combined loading case (2) ($b_2 = 0.01$) and axial compression alone ($b_2 = 0$), and under three sets of environmental conditions, i.e. 1: $T_U = 300$ K, $T_L = 300$ K, 2: $T_U = 600$ K, $T_L = 300$ K, and 3: $T_U = 900$ K, $T_L = 300$ K, are calculated and compared in Tables 3 and 4. In computation, the shell radius-to-thickness ratio $R/t = 300$ and 30, $\overline{Z} = 500$ and $T_0 = 300$ K. Also, three values of the volume fraction index N (= 0.2, 1.0 and 2.0) are considered. It is seen that, for the Si_3N_4/SUS304 cylindrical shell, the buckling loads are reduced with increases in temperature and with decreases in volume fraction index. In contrast, for the ZrO_2 /Ti–6Al–4V cylindrical shell, the buckling load is lower than that of the Si_3N_4 /SUS304 shell and erratic behavior can be observed in thermal environmental conditions 2 and 3. Therefore, Si_3N_4 /SUS304 cylindrical shells are considered in the parametric study only. Typical results are shown in Figs. 1–6. It is mentioned that in all figures $\overline{W}^*/t$ denotes the dimensionless maximum initial geometric imperfection of the shell.

Table 3
Comparisons of buckling loads (σ_{cr},q_{cr}) (in MPa) for Si_3N_4/SUS304 and ZrO_2/Ti–6Al–4V thin cylindrical shells subjected to combined axial and radial loads in thermal environments ($R/t = 300$, $\overline{Z} = 500$ and $T_0 = 300$ K)

Materials	N	$T_U = 300$ K, $T_L = 300$ K	$T_U = 600$ K, $T_L = 300$ K	$T_U = 900$ K, $T_L = 300$ K
Si_3N_4/SUS304	0.2	(400.462, 0) (394.361, 0.026) (126.572, 0.084) (0, 0.110)	(246.056, 0) (217.875, 0.015) (125.321, 0.084) (0, 0.109)	(183.825, 0) (99.964, 0.007) (125.530, 0.084) (0, 0.108)
	1.0	(461.427, 0) (425.393, 0.028) (145.110, 0.097) (0, 0.126)	(299.752 0) (280.897, 0.019) (140.988, 0.094) (0, 0.122)	(206.328, 0) (133.933, 0.009) (138.753, 0.093) (0, 0.119)
	2.0	(489.047, 0) (448.927, 0.030) (152.776, 0.102) (0, 0.132)	(328.230, 0) (312.739, 0.021) (147.709, 0.098) (0, 0.127)	(216.454, 0) (152.492, 0.010) (143.878, 0.096) (0, 0.123)
ZrO_2/Ti–6Al–4V	0.2	(204.983, 0) (189.945, 0.013) (64.795, 0.043) (0, 0.056)	(108.364 0) (89.714, 0.006) (61.430, 0.041) (0, 0.053)	(155.058, 0) (126.939, 0.008) (63.677, 0.042) (0, 0.052)
	1.0	(238.124, 0) (219.464, 0.015) (74.863, 0.050) (0, 0.065)	(112.236, 0) (31.805, 0.002) (66.923, 0.045) (0, 0.057)	(110.233, 0) (43.875, 0.003) (88.612, 0.059) (0, 0.057)
	2.0	(253.184, 0) (232.300, 0.015) (79.017, 0.053) (0, 0.068)	(156.431, 0) (32.430 0.002) (69.249, 0.046) (0, 0.058)	(248.205, 0) (93.396, 0.006) (105.830, 0.071) (0, 0.059)

Table 4
Comparisons of buckling loads (σ_{cr},q_{cr}) (in MPa) for Si_3N_4/SUS304 and ZrO_2/Ti–6Al–4V shear deformable cylindrical shells subjected to combined axial and radial loads in thermal environments ($R/t = 30$, $\overline{Z} = 500$ and $T_0 = 300$ K)

Materials	N	$T_U = 300$ K, $T_L = 300$ K	$T_U = 600$ K, $T_L = 300$ K	$T_U = 900$ K, $T_L = 300$ K
Si_3N_4/SUS304	0.2	(4110.570, 0) (3865.174, 2.577) (1248.377, 8.323) (0, 11.061)	(3790.912, 0) (3785.175, 2.523) (1230.890, 8.206) (0, 10.905)	(3493.155, 0) (3461.331, 2.308) (1216.803, 8.112) (0, 10.779)
	1.0	(4735.332, 0) (4420.001, 2.947) (1427.560, 9.571) (0, 12.648)	(4340.688, 0) (4281.516, 2.854) (1383.632, 9.224) (0, 12.258)	(3954.151, 0) (3930.001, 2.620) (1348.004, 8.987) (0, 11.942)
	2.0	(5018.193, 0) (4654.402, 3.103) (1503.253, 10.022) (0, 13.319)	(4589.686, 0) (4479.271, 2.986) (1447.439, 9.650) (0, 12.824)	(4163.306, 0) (4142.397, 2.762) (1402.305, 9.349) (0, 12.423)
ZrO_2/Ti–6Al–4V	0.2	(2103.800, 0) (1978.769, 1.319) (639.104, 4.261) (0, 5.662)	(1821.338 0) (1816.877, 1.211) (601.610, 4.011) (0, 5.330)	(1535.098, 0) (1430.851, 0.954) (588.425, 3.923) (0, 5.210)
	1.0	(2443.689, 0) (2279.964, 1.520) (736.376, 4.909) (0, 6.524)	(1779.783, 0) (1745.206, 1.163) (642.136, 4.281) (0, 5.688)	(2371.815, 0) (1842.126, 1.228) (609.899, 4.066) (0, 5.385)
	2.0	(2597.907, 0) (2407.847, 1.605) (777.672, 5.184) (0, 6.890)	(1783.359, 0) (1727.501, 1.152) (658.553, 4.390) (0, 5.833)	(2399.151, 0) (1849.098, 1.233) (618.903, 4.126) (0, 5.455)

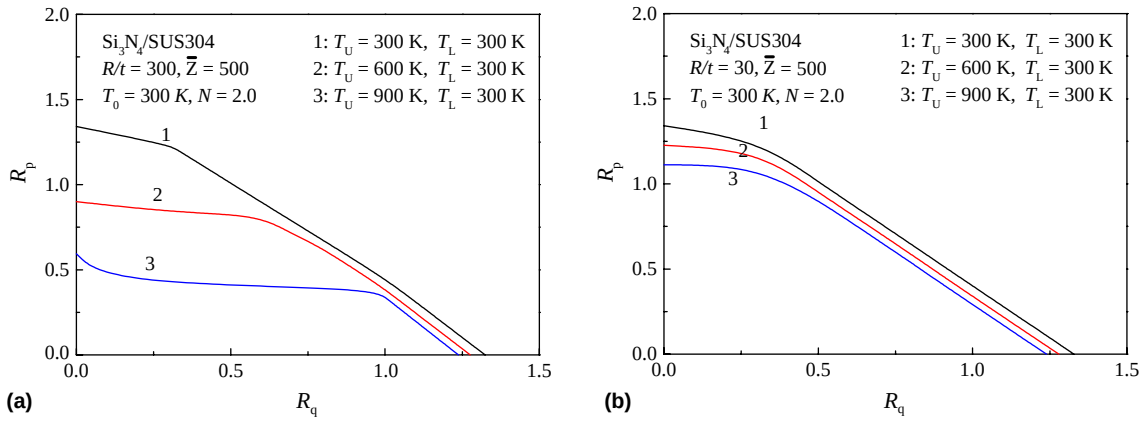

Fig. 1. Interaction buckling curves for Si_3N_4/SUS304 cylindrical shells subjected to combined axial and radial loads in three different sets of thermal environments: (a) thin shells; (b) shear deformable shells.

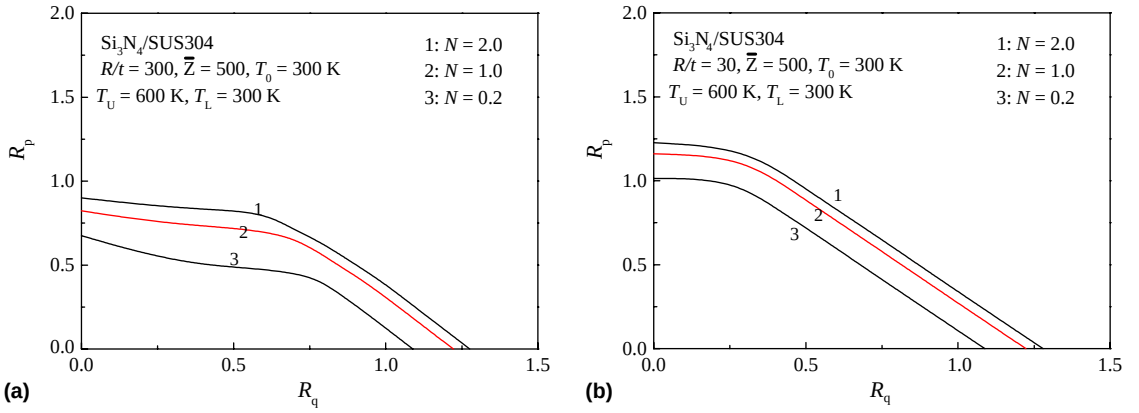

Fig. 2. Effect of volume fraction index N on the interaction buckling curves for Si_3N_4/SUS304 cylindrical shells subjected to combined axial and radial loads in thermal environments: (a) thin shells; (b) shear deformable shells.

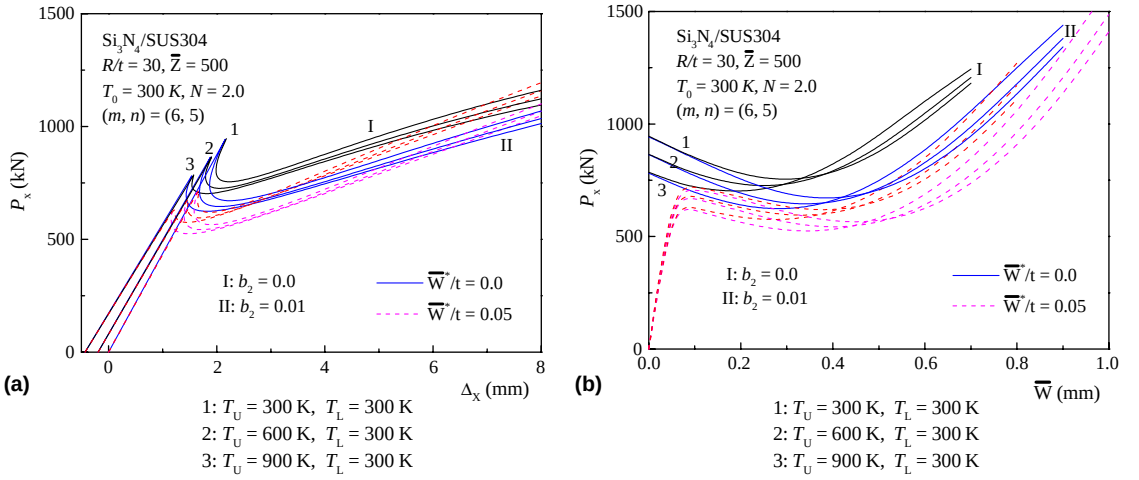

Fig. 3. Effect of temperature rise on the postbuckling behavior of Si_3N_4/SUS304 cylindrical shells subjected to axial compression combined with lateral pressure: (a) load-shortening; (b) load–deflection.

Fig. 1 shows the effects of temperature field on the interaction buckling curves of Si_3N_4/SUS304 thin and moderately thick cylindrical shells under combined loading cases, in which $R_x = q/q_{cr}$ and $R_y = \sigma_x/\sigma_{cr}$, where q_{cr} and σ_{cr} are critical buckling loads for the shell with $N = 0$ under lateral pressure alone or axial compression alone, and under environmental condition $T_U = 300$ K and $T_L = 300$ K. Then Fig. 2 shows the effects of volume fraction index on the interaction buckling curves of Si_3N_4/SUS304 thin and moderately thick cylindrical shells under environmental condition $T_U = 600$ K and $T_L = 300$ K. It is seen that the temperature field or volume fraction index has a significant effect on the shape of the interaction buckling curves. Of particular interest is the change from concave to convex behavior for the thin shell (see Figs. 1(a) and 2(a)).

Fig. 3 gives the postbuckling load-shortening and load–deflection curves for perfect ($\overline{W}^*/t = 0$) and imperfect ($\overline{W}^*/t = 0.05$), Si_3N_4/SUS304 moderately thick cylindrical shells ($R/t = 30$) with volume fraction index $N = 2.0$ under combined loading case (2) with the load-proportional parameter $b_2 = 0.0$ (referred to

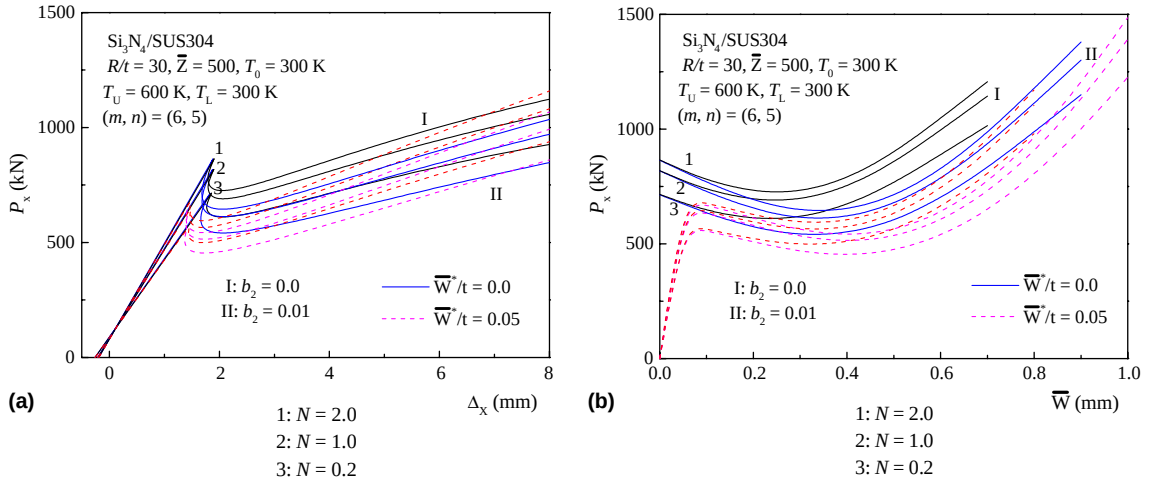

Fig. 4. Effect of volume fraction index N on the postbuckling behavior of Si_3N_4/SUS304 cylindrical shells subjected to axial compression combined with lateral pressure: (a) load-shortening; (b) load–deflection.

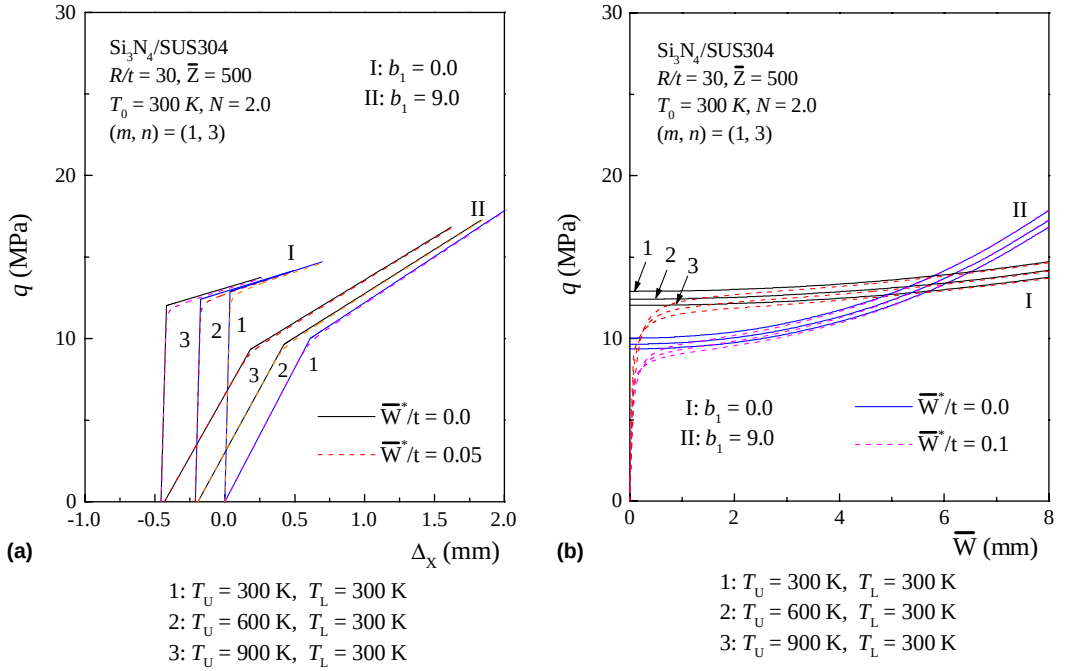

Fig. 5. Effect of temperature rise on the postbuckling behavior of Si_3N_4/SUS304 cylindrical shells subjected to hydrostatic pressure combined with axial compression: (a) load-shortening; (b) load–deflection.

as I) and 0.01 (referred to as II), and under three sets of thermal environmental conditions. It can be seen that the well-known "snap-through" behavior of shells occurs and the imperfection sensitivity can be predicted. Note that the postbuckling equilibrium path of the FGM shell is similar to that of the shell made

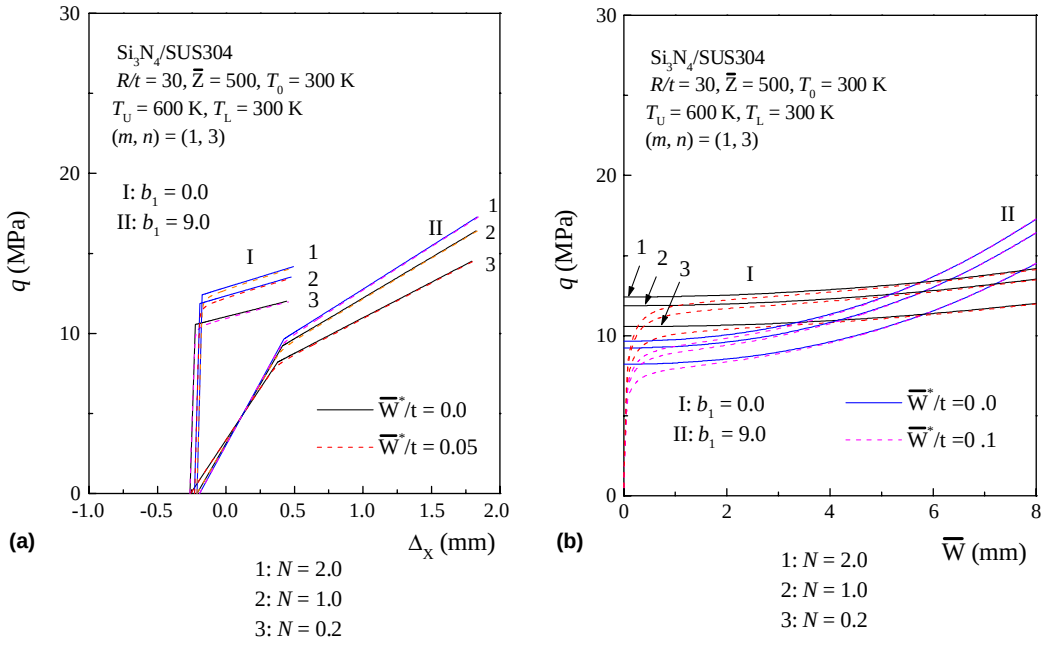

Fig. 6. Effect of volume fraction index N on the postbuckling behavior of Si_3N_4/SUS304 cylindrical shells subjected to hydrostatic pressure combined with axial compression: (a) load-shortening; (b) load–deflection.

from homogeneous isotropic materials. Clearly the buckling loads are reduced with increases in temperature, and the postbuckling load–deflection curve becomes significantly lower when $\overline{W}/t < 0.4$.

Fig. 4 gives the postbuckling load-shortening and load–deflection curves for perfect and imperfect, Si_3N_4/SUS304 moderately thick cylindrical shells with different values of volume fraction index $N(=0.2,\ 1.0$ and $2.0)$ under combined loading case (2) with the load-proportional parameter $b_2 = 0.0$ and 0.01, and under thermal environmental condition $T_U = 600$ K and $T_L = 300$ K. It can be seen that

Table 5
Imperfection sensitivity λ^* for Si_3N_4/SUS304 shear deformable cylindrical shells subjected to axial compression in thermal environments ($R/t = 30$, $\overline{Z} = 500$ and $T_0 = 300$ K)

Thermal environmental conditions	N	$\overline{W}^*/t$				
		0.0	0.05	0.1	0.15	0.20
$T_U = 300$ K, $T_L = 300$ K	0.0	1.0	0.774	0.641	0.548	0.479
	1.0	1.0	0.773	0.638	0.546	0.476
	2.0	1.0	0.770	0.636	0.543	0.475
$T_U = 600$ K, $T_L = 300$ K	0.0	1.0	0.827	0.684	0.586	0.512
	1.0	1.0	0.816	0.674	0.576	0.504
	2.0	1.0	0.810	0.669	0.572	0.500
$T_U = 900$ K, $T_L = 300$ K	0.0	1.0	0.862	0.734	0.628	0.549
	1.0	1.0	0.855	0.721	0.617	0.538
	2.0	1.0	0.852	0.714	0.610	0.534

the buckling loads are reduced with decreases in volume fraction index, and the postbuckling path becomes significantly lower as N decreases.

Figs. 5 and 6 show, respectively, the effects of temperature field and volume fraction index on the postbuckling behavior of the same cylindrical shells under combined loading case (1) with $a = 1$ (hydrostatic pressure combined with axial compression) and the load-proportional parameter $b_1 = 0.0$ and 9.0. It is seen that an increase in pressure is usually required to obtain an increase in deformation, and the postbuckling equilibrium path is stable for both perfect and imperfect shells, and the shell structure is virtually imperfection-insensitive.

Table 5 shows imperfection sensitivity of Si_3N_4/SUS304 moderately thick cylindrical shell with different values of volume fraction index N subjected to pure axial compression and under three sets of thermal environmental conditions. Here, λ^* is the maximum value of σ_x for the imperfect shell, made dimensionless by dividing by the critical value of σ_x for the perfect shell. These results show that the imperfection sensitivity of the shell becomes weaker as the temperature change increases. They also show that the volume fraction index N only has a small effect on the imperfection sensitivity of the FGM cylindrical shell.

5. Concluding remarks

This paper give the first theoretical postbuckling analysis of shear deformable FGM cylindrical shells subjected to combined axial and radial mechanical loads in thermal environments. The formulations are based on a higher order shear deformation shell theory with von Kármán–Donnell-type of kinematic nonlinearity and, therefore, the transverse shear deformation is accounted for. Heat conduction and temperature-dependent material properties are both taken into account. Numerical results are for Si_3N_4/SUS304 and ZrO_2/Ti–6Al–4V cylindrical shells. In effect, the results provide information about postbuckling behavior of FGM shells for different proportions of the ceramic and metal under different sets of environmental conditions. The results reveal that the temperature field and volume fraction distribution have a significant effect on the postbuckling behavior, but they have a small effect on the imperfection sensitivity of the FGM shell under combined loading conditions.

Acknowledgement

The support for this work, provided by the National Natural Science Foundation of China under Grant 50375091, and the invitation fellowship of JSPS is gratefully acknowledged.

Appendix A

In Eq. (22) [with C is defined as in Eq. (8b)]

$$A_x^{\mathrm{T}} = \frac{t}{1-v}\left\{[\alpha_{\mathrm{m}}(T_{\mathrm{L}}) - \alpha_{\mathrm{c}}(T_{\mathrm{U}})][E_{\mathrm{m}}(T_{\mathrm{L}}) - E_{\mathrm{c}}(T_{\mathrm{U}})]\frac{1}{2N+1} + (\alpha_{\mathrm{c}}(T_{\mathrm{U}})[E_{\mathrm{m}}(T_{\mathrm{L}}) - E_{\mathrm{c}}(T_{\mathrm{U}})]\right.$$
$$\left. + E_{\mathrm{c}}(T_{\mathrm{U}})[\alpha_{\mathrm{m}}(T_{\mathrm{L}}) - \alpha_{\mathrm{c}}(T_{\mathrm{U}})])\frac{1}{N+1} + \alpha_{\mathrm{c}}(T_{\mathrm{U}})E_{\mathrm{c}}(T_{\mathrm{U}})\right\} \quad (\text{for } T_1 = 0) \tag{A.1a}$$

$$A_x^{\mathrm{T}} = \frac{t}{1-\nu}\frac{T_{\mathrm{U}}-T_0}{T_1}\left\{[\alpha_{\mathrm{m}}(T_{\mathrm{L}})-\alpha_{\mathrm{c}}(T_{\mathrm{U}})][E_{\mathrm{m}}(T_{\mathrm{L}})-E_{\mathrm{c}}(T_{\mathrm{U}})]\frac{1}{2N+1}+(\alpha_{\mathrm{c}}(T_{\mathrm{U}})[E_{\mathrm{m}}(T_{\mathrm{L}})-E_{\mathrm{c}}(T_{\mathrm{U}})]\right.$$
$$\left.+E_{\mathrm{c}}(T_{\mathrm{U}})[\alpha_{\mathrm{m}}(T_{\mathrm{L}})-\alpha_{\mathrm{c}}(T_{\mathrm{U}})])\frac{1}{N+1}+\alpha_{\mathrm{c}}(T_{\mathrm{U}})E_{\mathrm{c}}(T_{\mathrm{U}})\right\}$$
$$+\frac{t}{1-\nu}\frac{T_{\mathrm{L}}-T_{\mathrm{U}}}{CT_1}\left\{[\alpha_{\mathrm{m}}(T_{\mathrm{L}})-\alpha_{\mathrm{c}}(T_{\mathrm{U}})][E_{\mathrm{m}}(T_{\mathrm{L}})-E_{\mathrm{c}}(T_{\mathrm{U}})]\right.$$
$$\times\left[\frac{1}{2N+2}-\frac{\kappa_{\mathrm{mc}}}{(N+1)(3N+2)\kappa_{\mathrm{c}}}+\frac{\kappa_{\mathrm{mc}}^2}{(2N+1)(4N+2)\kappa_{\mathrm{c}}^2}-\frac{\kappa_{\mathrm{mc}}^3}{(3N+1)(5N+2)\kappa_{\mathrm{c}}^3}\right.$$
$$\left.+\frac{\kappa_{\mathrm{mc}}^4}{(4N+1)(6N+2)\kappa_{\mathrm{c}}^4}-\frac{\kappa_{\mathrm{mc}}^5}{(5N+1)(7N+2)\kappa_{\mathrm{c}}^5}\right]+(\alpha_{\mathrm{c}}(T_{\mathrm{U}})[E_{\mathrm{m}}(T_{\mathrm{L}})-E_{\mathrm{c}}(T_{\mathrm{U}})]$$
$$+E_{\mathrm{c}}(T_{\mathrm{U}})[\alpha_{\mathrm{m}}(T_{\mathrm{L}})-\alpha_{\mathrm{c}}(T_{\mathrm{U}})])\left[\frac{1}{N+2}-\frac{\kappa_{\mathrm{mc}}}{(N+1)(2N+2)\kappa_{\mathrm{c}}}+\frac{\kappa_{\mathrm{mc}}^2}{(2N+1)(3N+2)\kappa_{\mathrm{c}}^2}\right.$$
$$\left.-\frac{\kappa_{\mathrm{mc}}^3}{(3N+1)(4N+2)\kappa_{\mathrm{c}}^3}+\frac{\kappa_{\mathrm{mc}}^4}{(4N+1)(5N+2)\kappa_{\mathrm{c}}^4}-\frac{\kappa_{\mathrm{mc}}^5}{(5N+1)(6N+2)\kappa_{\mathrm{c}}^5}\right]+\alpha_{\mathrm{c}}(T_{\mathrm{U}})E_{\mathrm{c}}(T_{\mathrm{U}})$$
$$\times\left[\frac{1}{2}-\frac{\kappa_{\mathrm{mc}}}{(N+1)(N+2)\kappa_{\mathrm{c}}}+\frac{\kappa_{\mathrm{mc}}^2}{(2N+1)(2N+2)\kappa_{\mathrm{c}}^2}-\frac{\kappa_{\mathrm{mc}}^3}{(3N+1)(3N+2)\kappa_{\mathrm{c}}^3}+\frac{\kappa_{\mathrm{mc}}^4}{(4N+1)(4N+2)\kappa_{\mathrm{c}}^4}\right.$$
$$\left.\left.-\frac{\kappa_{\mathrm{mc}}^5}{(5N+1)(5N+2)\kappa_{\mathrm{c}}^5}\right]\right\}\quad(\text{for } T_1\neq 0) \tag{A.1b}$$

and in Eqs. (41)–(43)

$$\Theta_1 = \frac{1}{C_3}\left[C_4+\frac{1}{\gamma_{24}}(1-\frac{1}{2}a_1\gamma_5)\lambda_q^{(2)}\right]$$

$$\Theta_2 = \frac{1}{\gamma_{24}}[(\gamma_{T2}-\gamma_5\gamma_{T1})T_1]\varepsilon-\frac{1}{\gamma_{24}}\left(1-\frac{1}{2}a\gamma_5\right)\lambda_q^{(0)}$$

$$\lambda_q^{(0)} = \left\{\frac{\gamma_{24}m^4}{C_1(1+\mu)g_{06}}+\frac{\gamma_{24}m^2}{C_1(1+\mu)^2}\frac{g_{05}+(1+\mu)g_{07}}{g_{06}}\varepsilon+\frac{1}{\gamma_{14}C_1(1+\mu)}\left[g_{08}+\gamma_{14}\gamma_{24}\frac{g_{05}}{g_{06}}\frac{(1+\mu)g_{07}-\mu g_{05}}{(1+\mu)^2}\right]\right.$$
$$\left.\times\left[1-\frac{\mu g_{05}}{(1+\mu)m^2}\varepsilon\left(1-\frac{\mu g_{05}}{(1+\mu)m^2}\varepsilon\right)\right]\varepsilon^2\right\}$$

$$\lambda_q^{(2)} = \frac{1}{4}\frac{m^4n^2\beta^2}{g_{06}}\left\{4\gamma_{24}(1+\mu)+\frac{1}{4}\frac{\gamma_{24}g_{06}g_{13}}{n^2\beta^2C_1}(1+2\mu)-\frac{\gamma_{24}n^2\beta^2g_{06}}{C_1(1+\mu)g_{06}-2a_1m^6g_{10}}\right.$$
$$\left.\times\left[2(1+\mu)^2+\frac{1}{2}\frac{a_1m^2}{C_1}(1+2\mu)+2\frac{S_4}{g_{06}}\right]\right\}$$

$$\delta_q^{(0)} = \frac{1}{\gamma_{24}}\left[\left(\frac{1}{2}a_1\gamma_{24}^2-\gamma_5\right)+\frac{2}{\pi}\frac{\gamma_5}{\gamma_{24}}\left(1-\frac{1}{2}a_1\gamma_5\right)(\vartheta b_{01}^{(5/2)}-\phi b_{10}^{(5/2)})\varepsilon^{1/2}\right]\lambda_q$$
$$+\left[\frac{1}{\pi(3)^{3/4}\gamma_{24}^2}\frac{b_{11}}{\vartheta}\left(1-\frac{1}{2}a_1\gamma_5\right)^2\varepsilon\right]\lambda_q^2$$

$$\delta_q^{(2)} = \frac{1}{32}(3)^{3/4}\left[m^2(1+2\mu)\varepsilon^{-3/2} - 2g_{05}\varepsilon^{-1/2} + \frac{g_{05}^2}{m^2}\varepsilon^{1/2}\right]$$

$$\delta_q^{(T)} = \frac{(3)^{3/4}}{4\gamma_{24}}\varepsilon^{-1/2}\left[\left(\gamma_{24}^2\gamma_{T1} - \gamma_5\gamma_{T2}\right)T_1\right]$$

$$S_4 = g_{06}(1+2\mu) + 8m^4(1+\mu)g_{10}, \quad S_5 = g_{06}C_1(1+\mu) - 2a_1m^6g_{10}$$

$$C_1 = n^2\beta^2 + \frac{1}{2}a_1m^2, \quad C_3 = 1 - \frac{g_{05}}{m^2}\varepsilon$$

$$C_4 = \frac{1}{8}n^2\beta^2(1+2\mu) + \frac{1}{8}n^2\beta^2C_1(1+\mu)\frac{S_4}{S_5} - \frac{1}{4}C_1(1+\mu)^2$$

and in Eqs. (50)–(52)

$$\Theta_3 = \frac{1}{C_3}\left[\gamma_{14}\gamma_{24}\frac{m^4(1+\mu)}{16n^2\beta^2g_{09}g_{06}}\varepsilon^{-1} - \gamma_{14}\gamma_{24}\frac{m^2g_{11}}{32n^2\beta^2g_{09}} + \frac{2(\gamma_5-a_2)}{\gamma_{24}}\lambda_p^{(2)}\right]$$

$$\Theta_4 = \frac{1}{\gamma_{24}}(\gamma_{T2} - \gamma_5\gamma_{T1})T_1 + \frac{2(\gamma_5-a_2)}{\gamma_{24}}\lambda_p^{(0)}$$

$$\lambda_p^{(0)} = \frac{1}{2}C_2\left\{\frac{\gamma_{24}m^2}{(1+\mu)g_{06}}\varepsilon^{-1} + \gamma_{24}\frac{g_{05}+(1+\mu)g_{07}}{(1+\mu)^2g_{06}} + \frac{1}{\gamma_{14}(1+\mu)m^2}\left[g_{08} + \gamma_{14}\gamma_{24}\frac{g_{05}}{g_{06}}\frac{(1+\mu)g_{07} - \mu(2+\mu)g_{05}}{(1+\mu)^2}\right]\varepsilon\right.$$
$$\left. - \frac{\mu}{(1+\mu)^2}\frac{g_{05}}{\gamma_{14}m^4}\left[1 + \frac{g_{05}}{(1+\mu)m^2}\varepsilon\right]\left[g_{08} + \gamma_{14}\gamma_{24}\frac{g_{05}}{g_{06}}\frac{(1+\mu)g_{07}+g_{05}}{(1+\mu)^2}(2+\mu)\right]\varepsilon^2\right\}$$

$$\lambda_p^{(2)} = \frac{1}{8}C_2\left\{\gamma_{14}\gamma_{24}^2\frac{m^6(2+\mu)}{2g_{09}g_{06}^2}\varepsilon^{-1} + \gamma_{14}\gamma_{24}^2\frac{m^4}{2g_{09}g_{06}}\left[\frac{g_{05}}{g_{06}} + \frac{g_{07}}{g_{06}}(1+\mu) + g_{12}(1+\mu) - \frac{1}{1+\mu}g_{11}\right]\right.$$
$$- \frac{1}{4}\gamma_{24}m^2g_{13}(1+2\mu)\varepsilon + \gamma_{14}\gamma_{24}^2\frac{m^2g_{11}}{2g_{09}}\left[\frac{g_{05}}{g_{06}}\frac{1}{1+\mu} - \frac{g_{07}}{g_{06}} - g_{12}\right]\varepsilon$$
$$\left. + \gamma_{14}\gamma_{24}^2\frac{m^2g_{05}}{2g_{09}g_{06}}\left[\frac{2(1+\mu)^2 - (1+2\mu)}{2(1+\mu)^2}g_{14} + \frac{\mu}{1+\mu}\frac{g_{05}}{g_{06}}\right](2+\mu)\varepsilon + \gamma_{24}\frac{m^2n^4\beta^4}{g_{06}}\frac{S_2}{S_1}\varepsilon\right\}$$

$$\lambda_p^{(4)} = \frac{1}{128}C_2\gamma_{14}^2\gamma_{24}^3\frac{m^{10}(1+\mu)}{g_{09}^2g_{06}^3}\frac{S_3}{S_{13}}\varepsilon^{-1}$$

$$\delta_p^{(0)} = \frac{(1+ab_2)}{\gamma_{24}}\left[(\gamma_{24}^2 - a_2\gamma_5) - \frac{2}{\pi}\frac{\gamma_5(\gamma_5-a_2)}{\gamma_{24}}(\vartheta b_{01}^{(2)} - \phi b_{10}^{(2)})\varepsilon^{1/2}\right]\lambda_p + \left[\frac{b_{11}}{2\pi\vartheta}\frac{(a_2-\gamma_5)^2}{\gamma_{24}^2}(1+ab_2)^2\varepsilon^{1/2}\right]\lambda_p^2$$

$$\delta_p^{(2)} = \frac{1}{16}\left[m^2(1+2\mu)\varepsilon - 2g_{05}\varepsilon^2 + \frac{g_{05}^2}{m^2}\varepsilon^3\right]$$

$$\delta_p^{(4)} = \frac{1}{128}\left\{\frac{b_{11}}{32\pi\alpha}\gamma_{14}^2\gamma_{24}^2\frac{m^8(1+\mu)^2}{n^4\beta^4g_{09}^2g_{06}^2}\varepsilon^{-3/2} + m^2n^4\beta^4(1+\mu)^2\left(\frac{S_4}{S_1}\right)^2\varepsilon^3\right\}$$

$$\delta_p^{(T)} = \frac{1}{2\gamma_{24}}(\gamma_{24}^2\gamma_{T1} - \gamma_5\gamma_{T2})T_1$$

$$S_1 = g_{06}(1+\mu) - 4m^2C_2g_{10}$$

$$
\begin{aligned}
S_2 &= g_{06}[(4+9\mu+4\mu^2)+C_2(1+2\mu)]+8m^4(1+\mu)(2+\mu)g_{10}\\
S_3 &= g_{136}[C_9(1+3\mu+\mu^2)+C_5(4+2\mu)+(1+\mu)]+g_{06}[C_5(6+8\mu+2\mu^2)-(2\mu+3\mu^2+\mu^3)]\\
S_{13} &= g_{136}C_9-g_{06}(1+\mu)\\
C_2 &= \frac{m^2}{m^2+a_2n^2\beta^2},\quad C_5=\frac{m^2+5a_2n^2\beta^2}{m^2+a_2n^2\beta^2},\quad C_9=\frac{m^2+9a_2n^2\beta^2}{m^2+a_2n^2\beta^2}
\end{aligned}
\tag{A.2}
$$

in the above equations [with g_{ij} and g_{ijk} are defined as in Shen and Li (2002)]

$$
\begin{aligned}
b &= \left[\frac{\gamma_{14}\gamma_{24}\gamma_{320}^2}{g_{16}}\right]^{1/2},\quad d=\gamma_{14}\gamma_{24}\gamma_{320}\frac{g_{15}}{2g_{16}},\quad \vartheta=\left[\frac{b-d}{2}\right]^{1/2},\quad \phi=\left[\frac{b+d}{2}\right]^{1/2}\\
a_{01}^{(1)} &= 1, a_{10}^{(1)}=\frac{\vartheta}{\phi}g_{17},\quad b_{01}^{(2)}=\gamma_{24}g_{19},\quad b_{10}^{(2)}=\gamma_{24}\frac{\vartheta}{\phi}g_{20}\\
b_{11} &= \frac{1}{b}\left[(a_{10}^{(1)})^2\phi^2 b+a_{10}^{(1)}2\vartheta\phi d+(2\vartheta^4-\vartheta^2\phi^2+\phi^4)\right]
\end{aligned}
\tag{A.3}
$$

References

Batdorf, S.B., 1947. A simplified method of elastic-stability analysis for thin cylindrical shells. NACA TR-874.

Galletly, G.D., James, S., Kruzelecki, J., Pemsing, K., 1987. Interactive buckling test on cylinders subjected to external pressure and axial compression. Journal of Pressure Vessel Technology ASME 109, 10–18.

Kim, K.-S., Noda, N., 2002. A Green's function approach to the deflection of a FGM plate under transient thermal loading. Archive of Applied Mechanics 72, 127–137.

Noda, N., 1991. Thermal stresses in materials with temperature-dependent properties. Applied Mechanics Review 44, 383–397.

Reddy, J.N., Chin, C.D., 1998. Thermoelastical analysis of functionally graded cylinders and plates. Journal of Thermal Stresses 21, 593–626.

Reddy, J.N., Liu, C.F., 1985. A higher-order shear deformation theory of laminated elastic shells. International Journal of Engineering Science 23, 319–330.

Shahsiah, R., Eslami, M.R., 2003a. Thermal buckling of functionally graded cylindrical shell. Journal of Thermal Stresses 26, 277–294.

Shahsiah, R., Eslami, M.R., 2003b. Functionally graded cylindrical shell thermal instability based on improved Donnell equations. AIAA Journal 41, 1819–1826.

Shen, H.S., 1997. Post-buckling analysis of imperfect stiffened laminated cylindrical shells under combined external pressure and axial compression. Computers and Structures 63, 335–348.

Shen, H.-S., 2001. Postbuckling of shear deformable cross-ply laminated cylindrical shells under combined external pressure and axial compression. International Journal of Mechanical Sciences 43, 2493–2523.

Shen, H.-S., 2002. Postbuckling analysis of axially-loaded functionally graded cylindrical shells in thermal environments. Composites Science and Technology 62, 977–987.

Shen, H.-S., 2003. Postbuckling analysis of pressure-loaded functionally graded cylindrical shells in thermal environments. Engineering Structures 25, 487–497.

Shen, H.-S., 2004. Thermal postbuckling behavior of functionally graded cylindrical shells with temperature-dependent properties. International Journal of Solids and Structures 41, 1961–1974.

Shen, H.-S., Chen, T.-Y., 1988. A boundary layer theory for the buckling of thin cylindrical shells under external pressure. Applied Mathematics and Mechanics 9, 557–571.

Shen, H.-S., Chen, T.-Y., 1990. A boundary layer theory for the buckling of thin cylindrical shells under axial compression. In: Chien, W.Z., Fu, Z.Z. (Eds.), Advances in Applied Mathematics and Mechanics in China. International Academic Publishers, Beijing, China, Vol. 2, pp. 155–172.

Shen, H.S., Chen, T.Y., 1991. Buckling and postbuckling of cylindrical shells under combined external pressure and axial compression. Thin-Walled Structures 12, 321–334.

Shen, H.-S., Li, Q.S., 2002. Thermomechanical postbuckling of shear deformable laminated cylindrical shells with local geometric imperfections. International Journal of Solids and Structures 39, 4525–4542.

Shen, H.S., Zhou, P., Chen, T.Y., 1993. Postbuckling analysis of stiffened cylindrical shells under combined external pressure and axial compression. Thin-Walled Structures 15, 43–63.

Tanigawa, Y., 1995. Some basic thermoelastic problems for nonhomogeneous structural materials. Applied Mechanics Review 48, 287–300.

Tanigawa, Y., Akai, T., Kawamura, R., Oka, N., 1996. Transient heat conduction and thermal stress problems of a nonhomogeneous plate with temperature-dependent material properties. Journal of Thermal Stresses 19, 77–102.

Touloukian, Y.S., 1967. Thermophysical Properties of High Temperature Solid Materials. McMillan, New York.